Aarhus University

Master's Thesis

Beta-decay of 8Li: beta-alpha correlations and final state distribution

Author:
Anders Holst Rasmussen

Supervisor:
Hans O. U. Fynbo

June 8, 2021

Contents

1 Introduction

1.1 Motivation

When Henri Becquerel first discovered radioactivity in the 1890's, a new branch of atomic physics was born, namely nuclear physics, which is the study of the atomic nuclei, their constituents and interactions. Over the years it has evolved quickly, first by the discovery of three different types of radiation by Curie and Rutherford, to the discovery of different nucleons, that the nucleus itself is made of. måske ref til Curie and Rutherford?

The technological advancements has made the study even more precise over the years, as the development of radioactive beams allow for the creation of specific short lived isotopes. This technique is known as Isotope Separation On-Line (ISOL), which was first developed in 1951 for the Copenhagen Cyclotron. Now the technology is available in many parts of the world, such as the IGISOL facility at the University of Jyväskylä in Finland [1]. Another important advancement is the development of very precise detectors, such as the Double Sided Silicon Detector (DSSD), which allows for a very high energy and spacial resolution, which can give a detailed analysis of both coincidence and kinematics.

This brings us onto the current experiment that I have analyzed in this thesis. At the IGISOL facility, the experiment I257 was carried out in august 2020. The objective of the experiment was to measure β-decays from ^{8}Li and ^{12}B, however, this thesis will only govern the ^{8}Li decay.
In precious studies, it has been shown that angle between the β-particle and the α-particles are very close to isotropic [2]. The study of the β-α correlation in ^{8}Li will therefore serve as a good indicator for the β-α correlation in

^{12}B, as the same setup will be used for both experiments.
A former student has previously made an in depth analysis of the mirror nucleus ^{8}B, which can be used to compare the excitation energy of ^{8}Be [3].

1.2 Nuclear decays

Lithium normally occurs stable as ^{6}Li and ^{7}Li, with the latter being the more abundant with 92.5% of all atoms. The longest living radioactive lithium isotope is ^{8}Li, with a half-life of 839 ms [4]. When ^{8}Li decays, it will do so by a β-decay, immediately followed by the α-α breakup of an intermediate exited state in ^{8}Be, which has a half life of 1×10^{-16} s. ^{8}Be is a constituent in the triple-alpha process in stellar astrophysics, and creates a bottleneck for the creation of heavier elements, because of its very short lifespan.

1.2.1 β-decay

Most light unstable nuclei will decay by either proton/neutron emission, or by a β-decay. Isotopes that lie close to the valley of stability will not decay by proton/neutron emission, but from a β-decay.
A β-decay is a weak interaction, which allows a quark in a proton or neutron to change flavor, by emitting a W boson. This leads to the creation of either an electron/antineutrino pair or a positron/neutrino pair:

$$\beta^+ : \quad p \rightarrow n + e^+ + \nu_e \tag{1.1}$$

$$\beta^- : \quad n \rightarrow p + e^- + \bar{\nu}_e. \tag{1.2}$$

Nuclei below the valley of stability will decay by β^-, while nuclei above decays by β^+.
The energy of these decays are given by their Q-values, neglecting the very small neutrino mass and the binding energy of the electrons gives:

$$Q_{\beta^+} = \left[m(^{A}_{Z}\mathrm{X}) - m(^{A}_{Z-1}\mathrm{X}')\right] c^2 \tag{1.3}$$

$$Q_{\beta^-} = \left[m(^{A}_{Z}\mathrm{X}) - m(^{A}_{Z+1}\mathrm{X}') - 2m_e\right] c^2, \tag{1.4}$$

where m is the mass of an atom with Z protons and A nucleons. The Q-values indicates the mass difference between the initial and final product., which can be either excitation energy or kinetic energy.
Not all β-decays are allowed. If the spin is unchanged, it is a Fermi transition, and if it changes it is a Gamow-Teller transition. An allowed decay is a transition with the change in orbital angular moment $\Delta L = 0$, and forbidden transitions have $\Delta L > 0$.
The nuclear part of the β-decay operator for an allowed decay is:

$$\mathcal{O}(\beta^{\pm}) = g_V \sum_{A}^{j=1} \tau_{\mp}(j) + g_A \sum_{A}^{j=1} \sigma(j)\tau_{\mp}(j), \tag{1.5}$$

where g_V is the weak vector coupling constant, $\tau_{\mp}$ is the isospin step operator, g_A is the weak axial coupling constant and σ is the Pauli spin matrices. The first term corresponds to the Fermi operator, and the second term to the Gamow-Teller operator. This raises some selection rules, that dictate that for a Fermi decay, spin, isospin and parity must not be changed, and for a Gamow-Teller transitions, $\Delta J = 0, \pm 1$, $\Delta T = 0, \pm 1$, and $\Delta \pi = 0$.
The selection rules then enforces that not every energy level is populated in ^{8}Be.

The ground state of ^{8}Li has spin, parity and isospin of $2^+; 1$, and a mass of $16.005\,\mathrm{MeV/c^2}$ more than the ground state of ^{8}Be, so it will only be able to populate states with lower energy than $16.005\,\mathrm{MeV}$, and states where the transition rules applies.
Looking at the states in ^{8}Be, there are only 3 states below the threshold of $16.005\,\mathrm{MeV}$, that is the ground state, first and second excited state. The ground state is a $0^+; 0$ state, with $\Delta J = 2$, which is forbidden given the selection rules.
The first excited state is a broad state at $3.03\,\mathrm{MeV}$ and $2^+; 0$, which gives $\Delta J = 0, \Delta \pi = 0$ and $\Delta T = 1$. This transition is valid within the selection rules, and is in fact the only state that will be populated in the decay.
The second excited state at $11.35\,\mathrm{MeV}$ is a $4^+; 0$, where $\Delta J = 2$, so the state

will not be populated either. The energy levels and properties can be seen on fig. 1.1.

1.2.2 α-decay

α-decay is another type of radioactive decay, where the nucleus emits an α-particle, and thereby decays into a different nucleus with the atomic number reduced by two. It has a Q-value of:

$$Q_\alpha = \left[m(^{A}_{Z}\mathrm{X}) - m(^{A-4}_{Z-2}\mathrm{X}') - m_\alpha\right] c^2. \tag{1.6}$$

Usually it is only elements heavier than nickel that can decay via this process, as the binding energy per nucleon decreases, and therefore becomes unstable towards spontaneous fission type processes. One of the only exceptions to this, is ^{8}Be, which is one of the only light nuclei that decays by α-decay.

1.2.3 Production of ^{8}Li

The production of ^{8}Li is rather crucial to the existance of the experiment, which is why the experiment had to be conducted at IGISOL HEJ SKRIV JYV. This facility is specialized in creating near stable isotopes of many elements.
In simple steps, the stable ^{7}Li is hit by a deuteron, where the neutron will stick to the the nucleus of ^{7}Li, and create ionized ^{8}Li. When it becomes ionized, it can be acellerated into a beam and shot at the target. The target is a thin carbon foil, where the ionized ^{8}Li will be stopped and lie. The target will transfer an electron to ^{8}Li, making it not ionized, and we are left with pure ^{8}Li just where we want it.

1.3 Structure of ^{8}Be

Figure 1.1 shows the excitation spectrum for ^{8}Be, with values from [4]. The spin, parity and isospin are written as $J^\pi;T$ for each level. 4 different states has been shown for ^{8}Be, where only the first excited state is the broad state

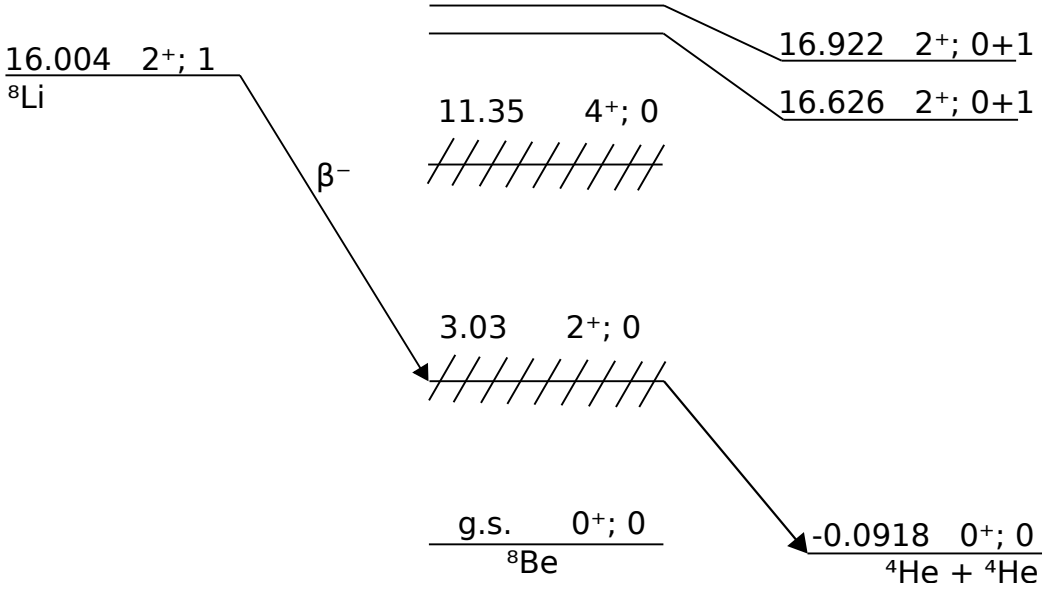

Figure 1.1: The decay scheme of ^{8}Li, and some notable excitation energies of ^{8}Be. Each level is labeled with the energy above the ^{8}Be ground state in MeV. Spin parity and isospin is noted as $J^\pi; T$. All information is from [4].

at 3.03 MeV. This state has conservation of spin and parity from ^{8}Li and is the only state that is allowed for the decay of ^{8}Li. Situated above is the broad state at 11.35 MeV, which does not conserve spin. Above that is a 16.626 MeV state, which conserves spin, parity and isospin, but lies energetically above ^{8}Li, so we would not expect that to shown in the data. It is still a quite relevant state, as the mirror nucleus ^{8}B $(2^+; 1)$ lies just above the energy at 17.979 MeV, and then has enough energy to populate this state, even though it is not very likely. Previous experiments made by the Aarhus subatomic group has examined the decay, and found only 5 counts populating this excitation level. But that should not show up when looking at the decay of ^{8}Li.

2 Analysis

2.1 The effects of the cuts

How does the cuts imposed in the previous chapter affect the data then? First we need to look at how the data looks, without any cuts. On fig. 2.1a the energy of the first α-particle ($E_{\alpha 1}$) is plotted against the energy of the second α-particle ($E_{\alpha 2}$). This gives us a nice view of what is considered α-particle pairs. There is a prominent line going diagonally through the graph, where both particles have around the same energy. This line is expected, as the α-particles will have close to equal energy, when decaying from ^{8}Be.
This means that there is a lot of particle pairs that have been identified as α-α, but properbly was α-noise, noise-noise, α-β or β-β pairs.
The lines occurring from $E_{\alpha 2} \approx 400\,\text{keV}$ are a clear example of a α-β pair. In this line, $\alpha 1$ has been identified correctly as a α-particle, which will have energies ranging from 500-6000 keV, whereas the the other particle has a more constant energy, corresponding to the energy a β-particle can deposit in a detector. So by doing no cuts at all, we are left with a lot of cases where we have no real control over what particle type we are dealing with.

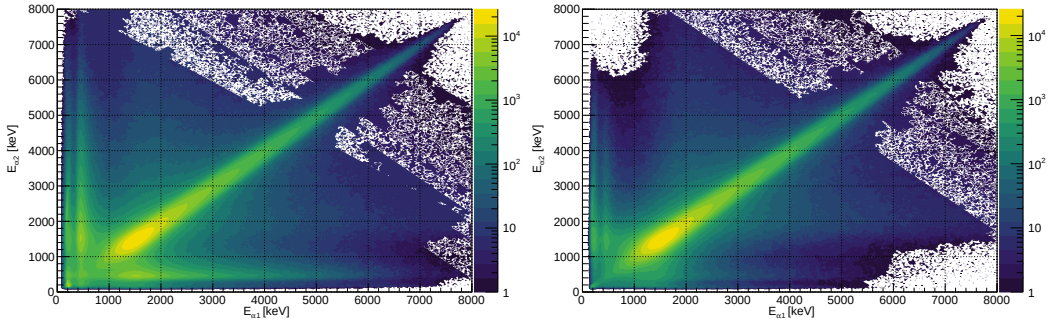

(a) No cuts on the data

(b) An angular cut. The angle between the two partcles must be greater than 160°.

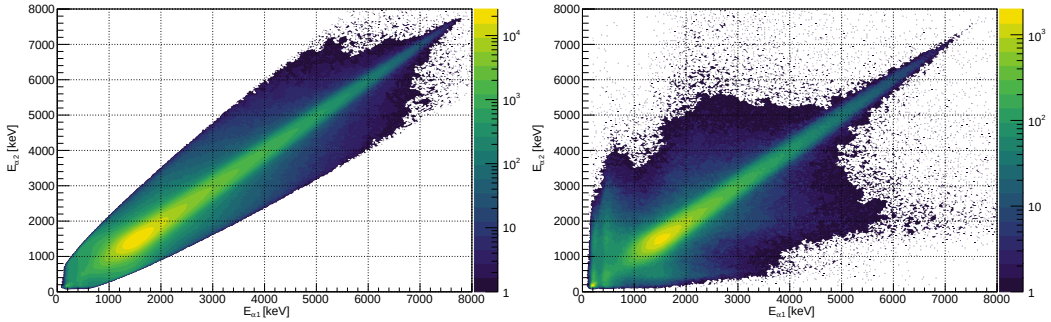

(c) A momentum cut. The total momentum of the particles must be less than 40 MeV/c

(d) A β-multiplicity cut. There must exist at least one β-particle and two α-particles in the event.

Figure 2.1: A collection of the different effects the cuts impose on the energy of the α-particles. On all the above figures, the energy of the first α-particle ($E_{\alpha 1}$) is plotted against the energy of the second α-particle ($E_{\alpha 2}$). The intensity scale is in logarithmic, to get a better view of all the different particle configurations.

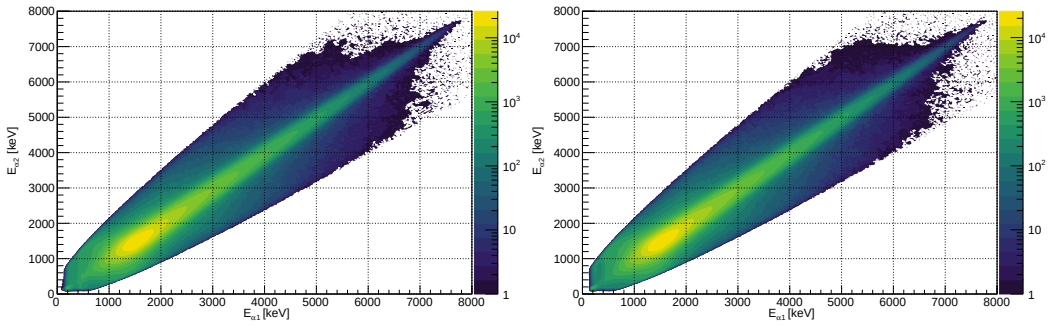

(a) Only moment **(b)** Ang and moment

Figure 2.2: A comparison of the momentum cut with and without the angular cut.

2.1.1 The effect of the angular cut

By imposing the angular cut, we get the first real reduction in data. If the angle between the two α-particles are less than $\cos(\theta) = -0.95 \approx 160°$, we sort away a good part of the β-α pairs, as seen on fig. 2.1b. But there are still a good portion of wrong pairs left, and we move on to impose a cut on the momentum of the particles.

2.1.2 The effect of the momentum cut

Again the aim is to sort the data, so that we can identify the particles. On fig. 2.1c the total momentum of the two particles has been limited to a maximum of 40 MeV/c. This cut sorts away all of the vertical and horizontal lines from a β-αpair. With this drastic cut, it looks like there is no use for the angular cut, which might be true. On figure 2.2 we can see the comparison of the effect of the momentum cut, with and without an angular cut. There does not seem to be a very large difference. Since momentum already takes the direction of the particles into account, as well as their energies, the angular cut will seem a bit redundant. However, we keep the angular cut on the data, as it will not take away any "good" measurements, but only some noise that slips through the multiplicity cut. Looking at fig. 2.4, we see the blue line as the momentum cut and the magenta line as the momentum and angular cut.

The two histograms lie very close to each other, except in the low energy ranger. Here we see a slight reduction in the magenta line, indicating that the pure angular cut will sort some β-particles from the data. It is therefor a justified cut to still impose on the data.

2.1.3 The effect of the multiplicity cut

The multiplicity of the β-particles should not interfere so much with the α-particles, but looking at fig. 2.1d, we see a drastic change in the pairs with energies far from each other. This is due to a general reduction in data. With the requirement that there must be one β-particle present in the event *and* that it must have hit either Det2 or DetD, we are left with a lot fewer measurements, which in turn gives a lower probability of noisy pairs.

2.1.4 The combined effect of all the cuts

By combining all of the cuts we are satisfied with the sorting of particles. On fig. 2.3 we see the effect of all the cuts. There is a very prominent line of particles with roughly the same energy. The line is thinner at higher energies, and widens as it goes towards lower energies. The reason for the widening, is the recoil energy from the β-decay. If the α-particles have low energy, they are more susceptible to other forces around it, and will lose a larger portion of their energy to the β-particle recoil.

On fig. 2.4 all the cuts are shown as individually, highlighting the effect that each cut provides. Here it is worth noting that not all β-particles have been successfully removed from the data. A slight peak at low energies still remain for the black line in the figure. This is also clear on fig. 2.3, where the there is a high intensity at the $\approx 200\,\text{keV}$ energy range.
An interesting effect that can be seen on the data, is the importance of the momentum cut. Looking the red and green line, we see a soft reduction in counts, different from the more rapid fall around 7 MeV. This is because there can be events where a particle will hit the detector, triggering it to measure, and before it turns completely off for detecting, another particle

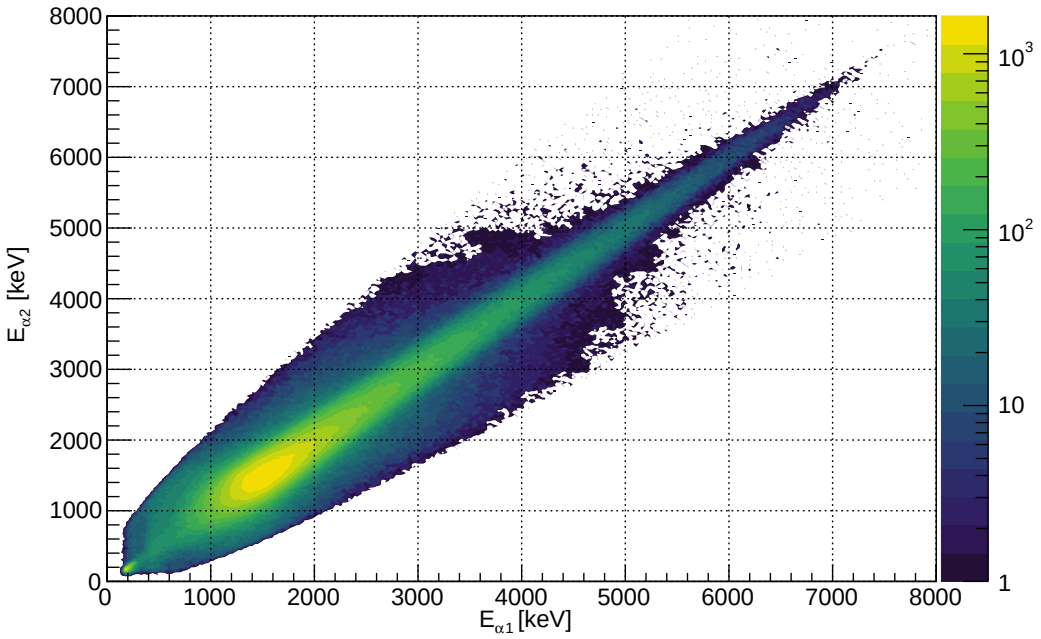

Figure 2.3: The energy of the first α-particle plotted against the energy of the second α-particle. All of the data reduction cuts are used here.

hits, and some of the the energies from both particles are measured as one particle.

So the momentum cut will also cut bad detection events away from the data in the high energy regime.

So far we have only considered that the α-particles are sorted correctly. But there is still a question for weather the β-particles will be clouded by wrong identifications. On fig. 2.5 we see the energy deposited in the two detectors that are capable of measuring β-particles, and the pad behind Det2. The energy from the pad and DetD, shows one peak around 400 keV and 300 keV, respectively. Det2 shows two peaks, one close to 400 keV, and one close to 800 keV. This is rather interesting, as we do not expect β-particles to deposit two different energies. Both detectors and the pad where 1000 μm thick, so we expect that the energy deposited would be roughly the same.

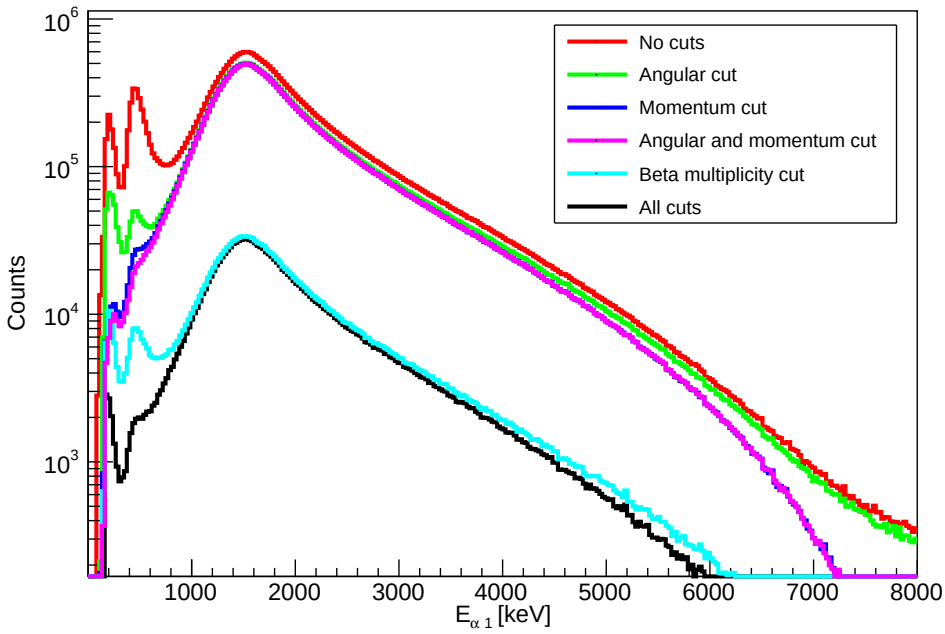

Figure 2.4: A comparison of all the cuts, with the energy of one α-particle shown.

2.2 The excitation energy of ^{8}Be

With the α-particles sorted correctly, we can start to look at the excitation energy of ^{8}Be. As mentioned in section 1.2.1 the β-decay of ^{8}Li will populate a broad exited state of ^{8}Be. This will give a more wide peak than we normally see in α-decays. On fig. 2.6 the energy sum of the α-particles has been plotted as the blue line. The peak lies closely to the mean energy of the exited state of 3.03 MeV, and then has a long tail all the way up to the around 16 MeV. At the low end of the spectra, there is a small peak just before the beginning of the main peak. This is the reminiscence of low energy β-β pairs that have not been sorted in the data. We will not worry too much about this, as the interesting properties of the spectra lies at higher energies than the main peak.

The green line is a fit made to another experiment by Bhattacharya [5]. The fitted green line has been multiplied by 70 as to better compare the two plots.

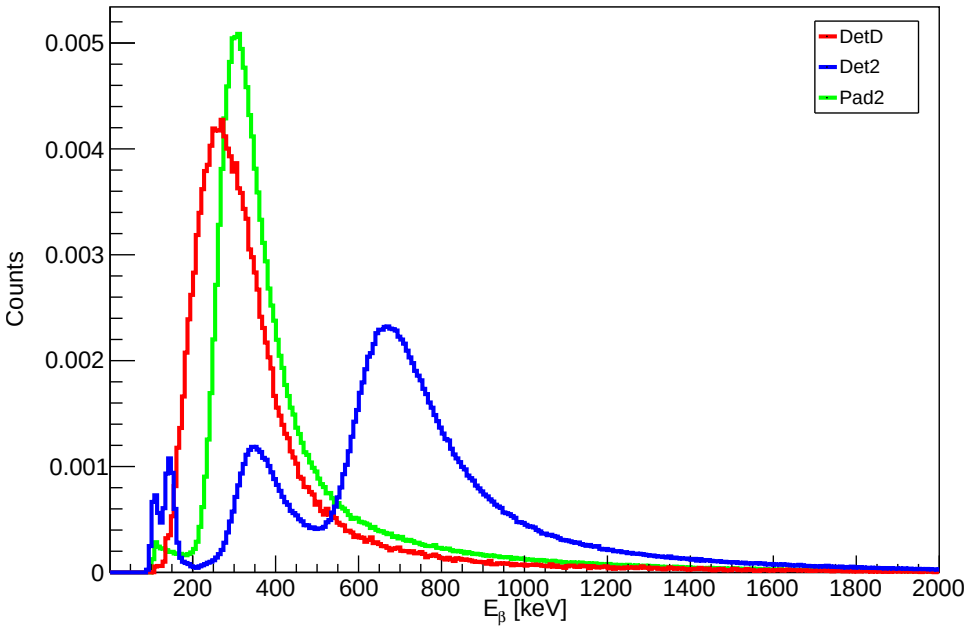

Figure 2.5: Energy deposited by β-particles in Det2 (blue), DetD (red) and Pad2 (green). PadD has been omitted, due to an error in the pad.

The plots differ a lot in the low energy range, as the β-particle contribution is rather prominent. But around the peak and at higher energy, the fit and our data follows nicely. At the very end, they differ again, as there seem to be some noise in our data, since the counts are too low to be considered otherwise.

2.3 Angular efficiency of the setup

Since the detectors are unable to cover the entire solid angle, there will always be some mutual angles that are more likely to be measured. If we only look at one detector, a very large number of angles are not covered, but small mutual angles such as $\theta \approx 0$, are very easy to measure, as it is just a measurement of two particles in the same pixel. This effect becomes apparent on fig. 2.7, where the angular efficiency is shown for Det2. For a single detector, there cannot be angles of $\theta = 90$ and higher, as the detector is flat. In this

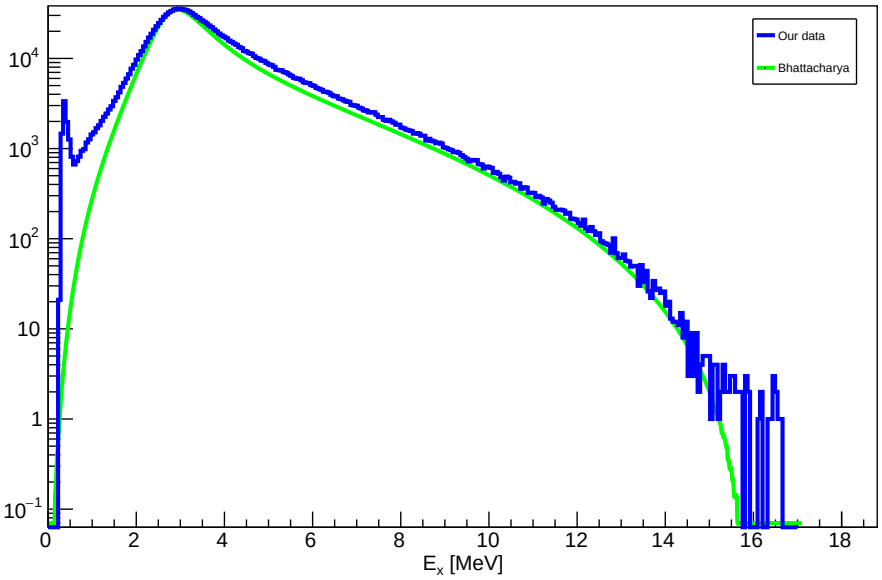

Figure 2.6: A comparison between the spectra of the excited state in ^{8}Be from this experiment(blue), and a fit found by Bhattacharya [5] (green).

detector, the lowest angle found was $\theta = 77°$.

In this setup however, we have a cube of square detectors, who's normal vectors are all pointing in towards target at the center. This gives a much larger coverage of all mutual angles. The placement of the detectors gives that angles around $\theta \approx 90°$ are also very favored. This makes sense, almost no matter what pixel was hit, there is a corresponding pixel 90° to both sides. In the same way, will there always be a corresponding pixel $\approx 180°$ from each pixels. This effect can be seen on fig. 2.8.
This histogram was created by using the spacial coordinates of the entire setup. First the positions of each pixel in each detector was found. Then two loops running over each pixel pair i, j, finds the angle between these pixels and saves it jeg ved ikke om man forstår dette hvis man ikke har været med til dette, så måske uddyb.

There is still a geometric effect that is not accounted for in the above analysis.

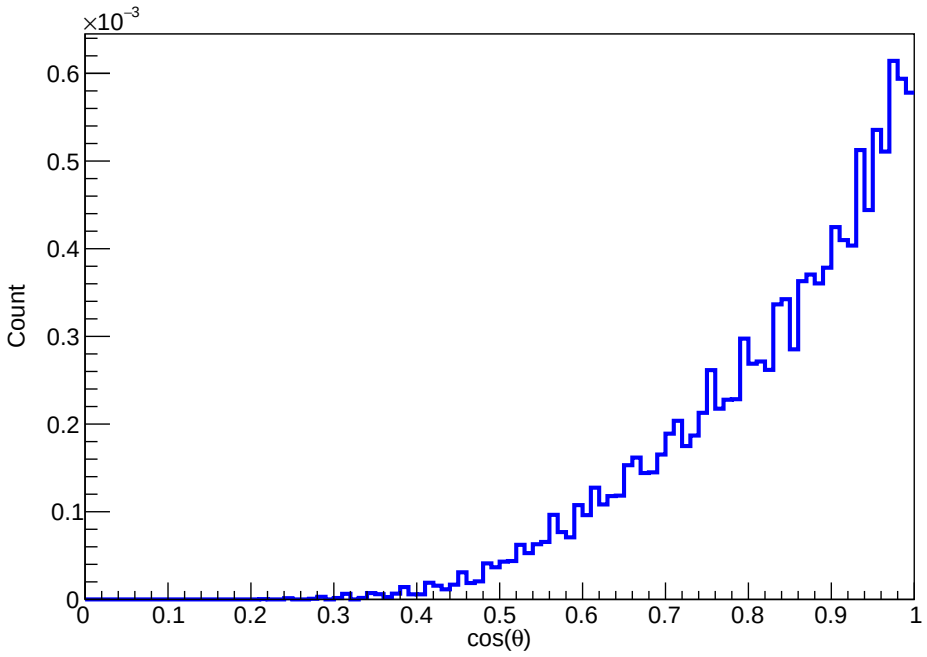

Figure 2.7: The angular efficiency of a single detector (Det2). For one flat detector, there can never be angles of 90° and higher.

We need to consider that not all pixels in the detector has the same effective area. The pixel furthest out in a detector will have a effective area smaller than the area of a pixel in the center. This effect can be seen on fig. 2.9a. Here we see that there is a much higher count of particles hitting the center of the detector, and fewer hitting the edges. A white line crossing through the middle is a defect strip, which did not measure anything. Sadly, some of the detectors had defect strips, but on a large scale it was not very noticeable måske lidt vagt.

To account for this effect det lyder som om der referes til effekten af de døde strips, each pixel will be associated with a corresponding area-efficiency (Eff_A). This is calculated as

$$\text{Eff}_A = \frac{A\cos(\theta)}{4\pi r^2}, \tag{2.1}$$

where r is the distance to the pixel, A is the area of the pixel and θ is the

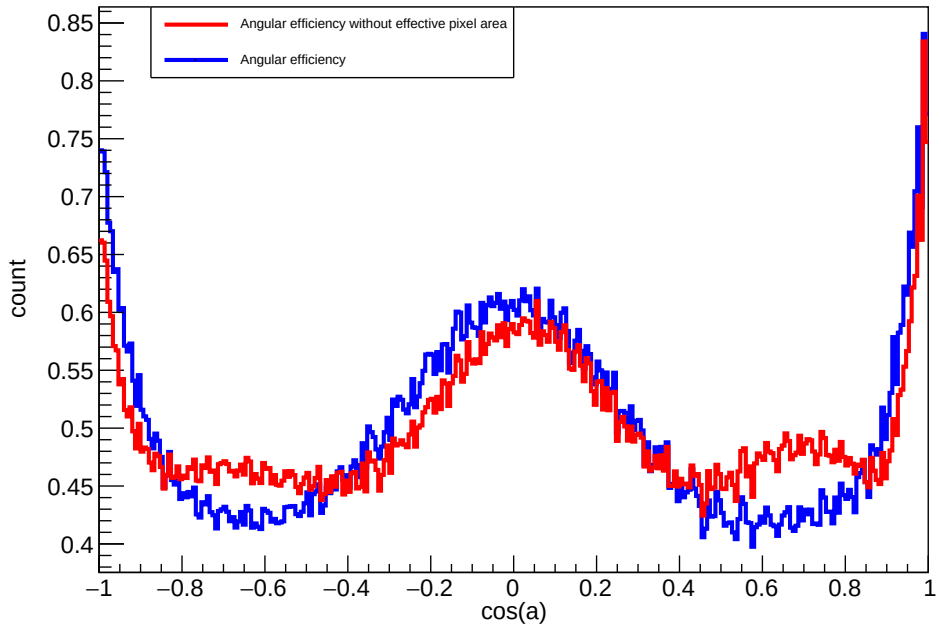

Figure 2.8: Two normalized histograms of the angular efficiency of the entire setup. The red histogram does not account for the effective area of a pixel. The blue is the true angular efficiency.

angle between the hit direction and the normal vector of the detector as shown on fig. 2.10. The area of all pixel is the same for all detectors, so the constants A and 4π can be ignored when comparing the efficiency.

On fig. 2.8 two histograms can be seen. The red line represents the angular efficiency of the setup, without accounting for the relative area of the pixels, while the blue line is a weighted histogram for the same angles, with each pixels relative area accounted for.

The form of the two histograms are quite similar around 1, 0 and -1 but in between there is a rather prominent difference. Therefore it is important that the effective area of the pixel is accounted for, when we in section 2.4 will look at the angular correlations of the β-particle in the setup.

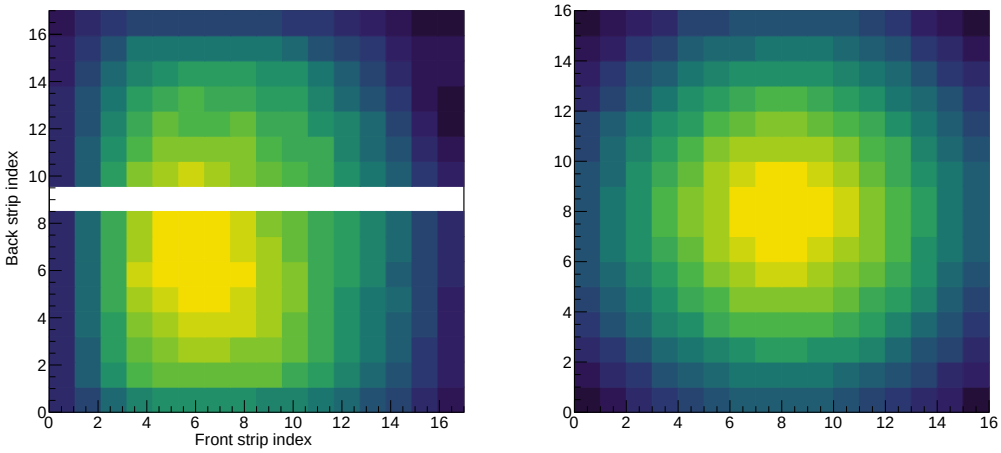

(a) A plot over the number of hits in each strip for Det2. The white line in the middle is a defect strip, that did not measure anything.

(b) A theoretical intensity Det2.

Figure 2.9

2.4 Angular correlations of α-particles and β-particles

From what we know in ref til beta = isotrop the β-particles must have an isotropic distribution. Since we only have two detectors in the setup that are capable of measuring β-particles, we cannot measure the angle from one particle to something constant, i.e. the beam. Therefore we measure the angle between both α-particles and the β-particles. This is done by first finding the angle between the first α-particle α_1 vinkel mellem alfa og hvad?, and create a histogram of this. Then the angle between the second α-particle α_2 is measured vinkel mellem alfa og hvad?, and a histogram is created. The two histograms are then added, to get the full picture of the mutual angles of the particles. This can be seen on fig. 2.11 as the green line.
The blue line in this figure is the angular efficiency for the specific case, where the α-particles can hit in any given detector, but the β-particles can only hit in the two specific detectors Det2 and DetD. The two histograms has both

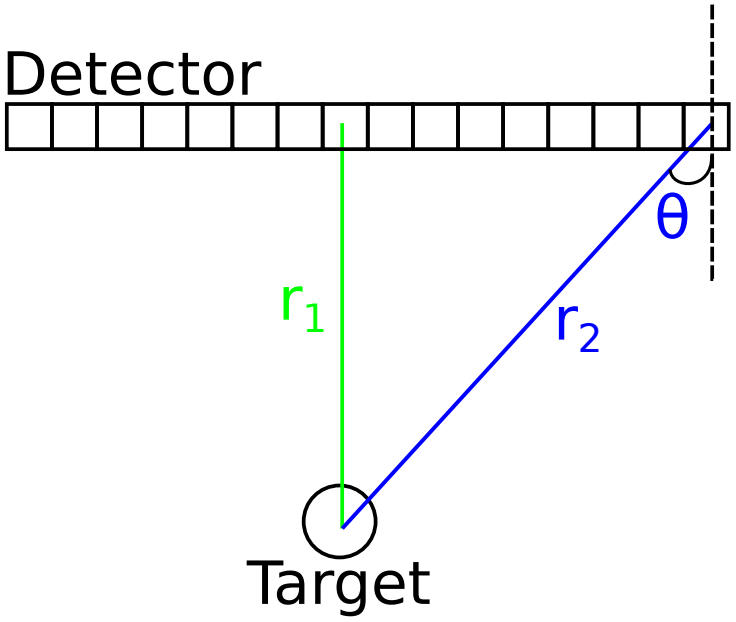

Figure 2.10: A illustration of two hits in different pixels. The blue hit will see a smaller effective area of the pixel by a factor determined by eq. (2.1) Måske tilføj "den blå retnmingsvektor projiceret på den stiplede linje bliver minder for større theta eller noget´. Denne figur er kommet i forkert rækkefølge

been normalized, for a better comparison. By dividing the two histograms with each other, we get a better comparison. If they where to be close to equal, we would see a flat curve. But what we see on fig. 2.12 is not very flat. There are small fluctuations in the line, which stems from the inaccuracy of calculated angular efficiency. But the main shape of the curve is at most time not around $y = 1$.

There are two different explanations as to why this might be. The first explanation is that the beam did not hit the target in the center. The calculated efficiency assumes that the beam hits precisely in the middle, but in any setup, there can be a few millimeters of errors.

By finding the angular efficiency of the setup, with different values for the center and comparing this to the measured angles, we have found a slight correction for the center of the beam. This can be seen on fig. 2.13a, where the beam has been moved to the coordinates $(-3, -3, 0)$, as opposed to the

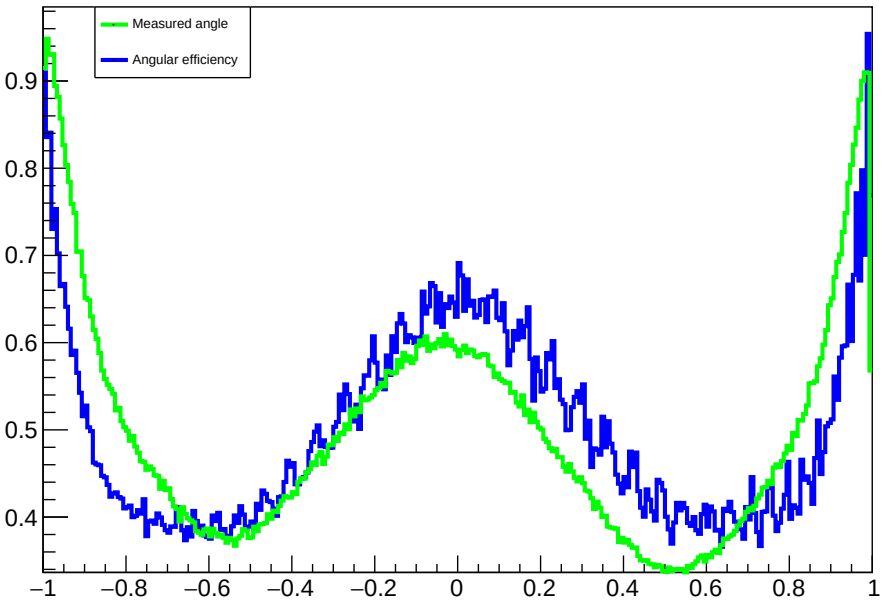

Figure 2.11: Some figure of the efficiency of the setup without efficiency of each pixel. anden figurtekst?

previous of $(0, 0, 0)$. The division fo the two histograms on fig. 2.13b shows a more stable line from $\cos(\theta) = -0.4$ to $\cos(\theta) = 0.4$, but the edges are still not very alike. Looking at $\cos(\theta) = 1$, we see a rapid fall, which indicates that we have measured a lot fewer parallel β and α-particles than the setup is designed to handle. This can be due to the fact that some of the strips where defect. The calculated angular efficiency does not know which strips where defect, and and will therefore have a lot higher efficiency for parallel particles. The defect strips will therefore also play a role in the grand scheme, and is a possible explanation as to why there is a difference in the calculated and the measured data.

Another effect that will sway the data, is the target holder. This device will provide a shadow over the top and bottom detector, and since one of the β-detectors are the bottom one, it will skew the data in a unforeseeable way.

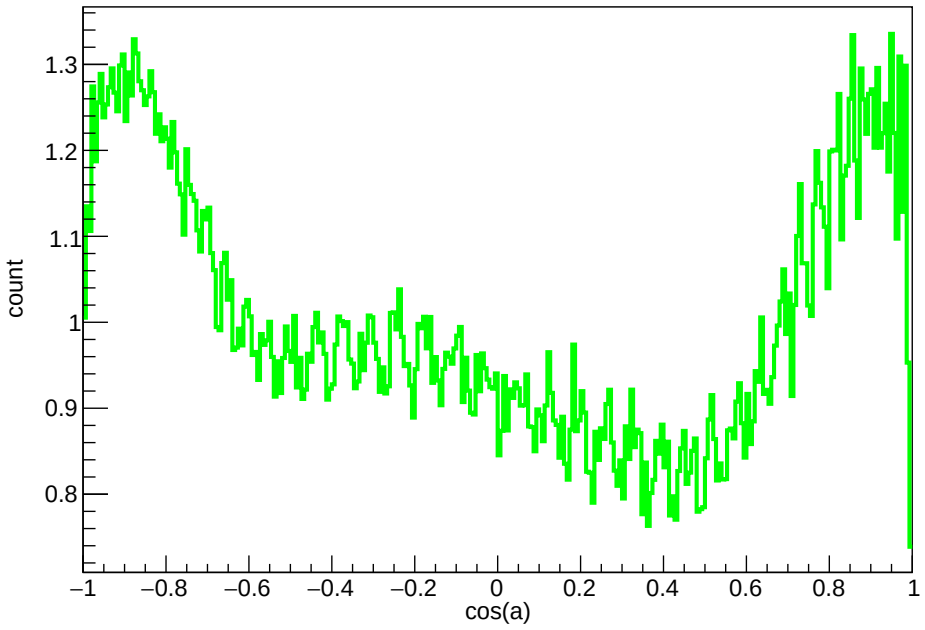

Figure 2.12: Data divided by the angular efficiency.

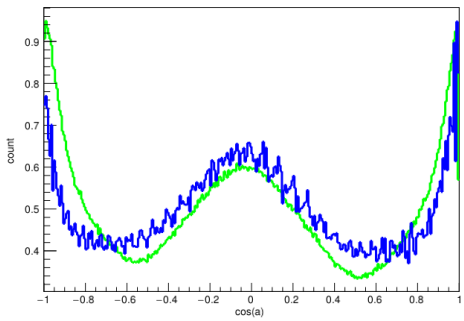

(a) The angular efficiency and the data, with a correction for the center of the beam.

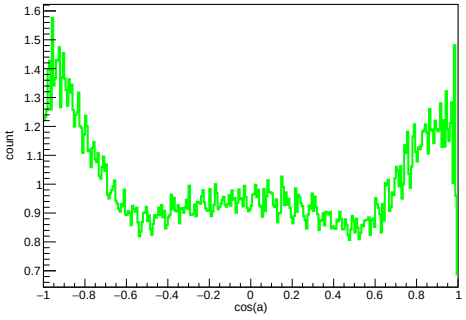

(b) Measured β-α-particle angular distribution divided by the calculated angular efficiency of the setup, with a correction for position of the beam.

Bibliography

[1] Igisol. https://www.jyu.fi/science/en/physics/research/infrastructures/accelerator-laboratory/nuclear-physics-facilities/the-exotic-nuclei-and-beams.

[2] R. E. Tribble and G. T. Garvey. Induced weak currents and $\beta^{\pm} - \alpha$ angular correlations in $a = 8$. *Phys. Rev. C*, 12:967–983, Sep 1975.

[3] Andreas Gad. An experimental study of ^{8}B beta decay. Master Thesis. Aarhus University, Department of Physics and Astronomy, 2018.

[4] D.R. Tilley, J.H. Kelley, J.L. Godwin, D.J. Millener, J.E. Purcell, C.G. Sheu, and H.R. Weller. Energy levels of light nuclei a=8,9,10. *Nuclear Physics A*, 745(3):155–362, 2004.

[5] M. Bhattacharya, E. G. Adelberger, and H. E. Swanson. Precise study of the final-state continua in ^{8}Li and ^{8}B decays. *Phys. Rev. C*, 73:055802, May 2006.